

*The Canadian Mineralogist*  
Vol. 42, pp. 1757-1769 (2004)

## PUTZITE, $(\text{Cu}_{4.7}\text{Ag}_{3.3})_{\Sigma 8}\text{GeS}_6$ , A NEW MINERAL SPECIES FROM CAPILLITAS, CATAMARCA, ARGENTINA: DESCRIPTION AND CRYSTAL STRUCTURE

WERNER H. PAAR<sup>§</sup>

*Department of Geography, Geology and Mineralogy, University of Salzburg, Hellbrunnerstrasse 34, A-5020 Salzburg, Austria*

ANDREW C. ROBERTS

*Geological Survey of Canada, 601 Booth Street, Ottawa, Ontario K1A 0E8, Canada*

PETER BERLEPSCH AND THOMAS ARMBRUSTER

*Laboratorium für chemische und mineralogische Kristallographie, Universität Bern, Freiestrasse 3, CH-3012 Bern, Switzerland*

DAN TOPA AND GEORG ZAGLER

*Department of Geography, Geology and Mineralogy, University of Salzburg, Hellbrunnerstrasse 34, A-5020 Salzburg, Austria*

### ABSTRACT

Putzite, chemically  $(\text{Cu}_{4.7}\text{Ag}_{3.3})_{\Sigma 8}\text{GeS}_6$ , was discovered in old dumps near the Rosario vein, Capillitas mining district, Department of Andalgalá, Catamarca Province, Argentina. The Capillitas diatreme is located within the Farallón Negro volcanic complex, which is host to large porphyry Cu–Au deposits (Bajo de la Alumbrera, Agua Rica) and genetically related epithermal vein-type deposits. The mineral assemblage that contains putzite is composed of bornite, chalcocite, sphalerite, tennantite, wittichenite, thalcosite, catamarcaite (IMA 2003–020), an undefined Cu–Fe–Zn–Ge sulfide possibly representing the Ge-dominant analogue of stannoidite, chalcopyrite, galena, luzonite and quartz. Putzite occurs as aggregates of anhedral grains, up to  $3 \times 1$  mm, embedded in a matrix of predominantly chalcocite with relics of bornite. The mineral is opaque, iron-black with a weak violet tint, has a metallic luster and a black streak. It is brittle, the fracture is irregular to subconchoidal (rarely splintery), and the cleavage, whose orientation is unknown, is distinct in polished sections.  $\text{VHN}_{50}$  ranges between 183 and 201 (mean 188)  $\text{kg/mm}^2$ , which corresponds to a Mohs hardness of about 3–3½. The density, 5.788  $\text{g/cm}^3$ , was calculated using the empirical formula and  $Z = 4$ . In plane-polarized reflected light in air, the mineral is pale rose to pale violet (in contrast with chalcocite), lacks internal reflections and is isotropic. The reflectance spectra in air and in oil are tabulated. The chemical composition, which was determined with an electron microprobe, shows weak variation from grain to grain. The average composition of one sample (four grains, 29 analyses) is: Cu 33.04, Ag 39.33, Ge 7.79, S 20.55, total 100.71 wt.%; another specimen yielded Cu 32.71, Ag 39.83, Ge 7.62, S 20.59, total 100.75 wt.%. This leads to empirical formulae (based on total atoms = 15) of  $(\text{Cu}_{4.78}\text{Ag}_{3.35})_{\Sigma 8.13}\text{Ge}_{0.99}\text{S}_{5.89}$  and  $(\text{Cu}_{4.73}\text{Ag}_{3.40})_{\Sigma 8.13}\text{Ge}_{0.97}\text{S}_{5.91}$ , respectively. The ideal formula,  $(\text{Cu}_{4.7}\text{Ag}_{3.3})_{\Sigma 8}\text{GeS}_6$ , requires: Cu 32.48, Ag 38.71, Ge 7.89, S 20.92, total 100.00 wt.%. Putzite is cubic, with a unit-cell parameter  $a$  refined from X-ray powder-diffraction data equal to 10.201(3) Å,  $V = 1061.5(6)$  Å<sup>3</sup>, space group  $F\bar{4}3m$  (216). The strongest seven X-ray powder-diffraction lines [ $d$  in Å( $hkl$ )] are: 5.896(30)(111), 3.074(60)(311), 2.943(100)(222), 2.083(30)(422), 1.962(50)(333), 1.805(70)(440) and 1.725(25)(531). The crystal structure of putzite was solved by direct methods to an  $R$  index of 5.97% for 259 observed reflections measured with  $\text{MoK}\alpha$  X-radiation. Close metal–metal contacts indicate Cu,Ag disorder. The structure description is based on regular polyhedra such as  $\text{GeS}_4$ ,  $\text{SCu}_6$ ,  $\text{SAg}_{12}$  and  $\text{SCu}_{12}$ , instead of the conventional discussion of various two-, three-, or four-fold coordinations around (disordered) Ag and Cu. Putzite belongs to the argyrodite group and is an Ag-rich variety of the synthetic inorganic compound  $\gamma$ - $\text{Cu}_8\text{GeS}_6$ . The mineral name honors Hubert Putz (b. 1973), who discovered the new species during field work in Catamarca, for his significant contribution to the mineralogy of germanium in the Capillitas deposit. The mineral and the mineral name have been approved by the Commission of New Minerals and Mineral Names, IMA (2002–024).

**Keywords:** putzite, new mineral species, copper silver germanium sulfide, electron-microprobe analyses, X-ray data, reflectance data, crystal structure, Rosario vein, Capillitas district, Farallón Negro complex, Catamarca Province, Argentina.

<sup>§</sup> E-mail address: werner.paar@sbg.ac.at

## SOMMAIRE

La putzite, dont la composition chimique est  $(\text{Cu}_{4.7}\text{Ag}_{3.3})_{\Sigma 8}\text{GeS}_6$ , est une nouvelle espèce minérale découverte dans des haldes près de la veine de Rosario, camp minier de Capillitas, département d'Andalgalá, province de Catamarca, en Argentine. La diatrème de Capillitas est située au sein du complexe volcanique de Farallón Negro, qui renferme des gisements volumineux de type Cu–Au associés à des systèmes porphyriques (Bajo de la Alumbreira, Agua Rica) et des gisements épithermaux en veines. L'assemblage de minéraux qui contient la putzite comprend bornite, chalcocite, sphalérite, tennantite, wittichenite, thalcosite, catamarcaïte (IMA 2003–020), un sulfure méconnu à Cu–Fe–Zn–Ge, possiblement l'analogue à dominance de Ge de la stannoidite, chalcopyrite, galène, luzonite et quartz. La putzite se présente en agrégats de grains xénomorphes atteignant  $3 \times 1$  mm, dans une matrice surtout faite de chalcocite avec reliques de bornite. Il s'agit d'un minéral opaque, noir-fer avec une légère teinte violacée, un éclat métallique et une rayure noire. Il est cassant, la fracture est irrégulière, voire subconchoïdale (rarement en échapes), et le clivage, dont l'orientation est méconnue, est distinct en sections polies. Les valeurs de  $\text{VHN}_{50}$  vont de 183 à 201 (en moyenne, 188)  $\text{kg/mm}^2$ , ce qui correspond à une dureté de Mohs d'environ 3–3½. La densité, 5.788  $\text{g/cm}^3$ , est calculée à partir de la formule empirique et  $Z = 4$ . En lumière réfléchie polarisée dans l'air, le minéral est rose pâle à violet pâle (par rapport à la chalcocite), dépourvu de réflexions internes, et isotrope. Nous fournissons les données spectrales de réflectance dans l'air et dans l'huile. La composition chimique, établie avec une microsonde électronique, varie légèrement d'un échantillon à l'autre. La composition moyenne d'un échantillon (quatre grains, 29 analyses) serait: Cu 33.04, Ag 39.33, Ge 7.79, S 20.55, pour un total de 100.71% (poids); un autre échantillon a donné Cu 32.71, Ag 39.83, Ge 7.62, S 20.59, pour un total de 100.75%. Ces données mènent aux formules empiriques (sur une base de 15 atomes) de  $(\text{Cu}_{4.78}\text{Ag}_{3.35})_{\Sigma 8.13}\text{Ge}_{0.99}\text{S}_{5.89}$  et  $(\text{Cu}_{4.73}\text{Ag}_{3.40})_{\Sigma 8.13}\text{Ge}_{0.97}\text{S}_{5.91}$ , respectivement. La formule idéale,  $(\text{Cu}_{4.7}\text{Ag}_{3.3})_{\Sigma 8}\text{GeS}_6$ , requiert: Cu 32.48, Ag 38.71, Ge 7.89, S 20.92, pour un total de 100.00%. La putzite est cubique, avec un paramètre réticulaire  $a$  affiné à partir des données en diffraction X sur poudre égal à 10.201(3) Å,  $V = 1061.5(6)$  Å<sup>3</sup>, groupe spatial  $F\bar{4}3m$  (216). Les sept raies les plus intenses du spectre de diffraction, méthode des poudres [ $d$  en Å(1)( $hkl$ )], sont: 5.896(30)(111), 3.074(60)(311), 2.943(100)(222), 2.083(30)(422), 1.962(50)(333), 1.805(70)(440) et 1.725(25)(531). Nous avons résolu la structure cristalline de la putzite par méthodes directes jusqu'à un résidu  $R$  de 5.97% en utilisant 259 réflexions observées mesurées avec un rayonnement  $\text{MoK}\alpha$ . Des distances rapprochées entre atomes métalliques indiquent un désordre Cu,Ag. La description de la structure est fondée sur des polyèdres réguliers tels  $\text{GeS}_4$ ,  $\text{SCu}_6$ ,  $\text{SAg}_{12}$  et  $\text{SCu}_{12}$ , au lieu d'une discussion conventionnelle de diverses coordinences (deux, trois ou quatre) autour des cations Ag et Cu (désordonnés). La putzite fait partie du groupe de l'argyrodite, et serait une variante riche en Ag du composé inorganique synthétique  $\gamma\text{-Cu}_8\text{GeS}_6$ . Le nom choisi honore Hubert Putz (né en 1973), qui a découvert la nouvelle espèce au cours de ses travaux de terrain à Catamarca, pour sa contribution importante à la minéralogie du germanium dans le gisement de Capillitas. Le minéral et son nom ont été approuvés par la Commission des Nouveaux Minéraux et des Noms de Minéraux, Association Minéralogique Internationale (2002–024).

(Traduit par la Rédaction)

**Mots-clés:** putzite, nouvelle espèce minérale, sulfure de cuivre, argent et germanium, données de microsonde électronique, données de diffraction X, données de réflectance, structure cristalline, veine de Rosario, district de Capillitas, complexe de Farallón Negro, province de Catamarca, Argentine.

## INTRODUCTION

The Capillitas district in the Department of Andalgalá, Catamarca Province, northwestern Argentina, is well known for its famous mining history. Local "indios" are considered to have been the first miners of gold from the alluvial deposits and outcrops. Later on, during the 17<sup>th</sup> and 18<sup>th</sup> centuries, Jesuit priests successfully mined gold. Since approximately 1850, private companies from Argentina and England were active in the district, and mined for copper, with gold and silver recovered as by-products. The mining terminated at the beginning of the 20<sup>th</sup> century; the rich portions of the veins were exhausted, and significant problems in beneficiation were encountered with the remaining complex ores at deeper levels of the veins. However, the Capillitas district still remains the source of magnificent gem-quality rhodochrosite, which had been mined for more than fifty years, particularly from the Ortiz mine.

As part of a bilateral project between the Austrian (FWF) and the Argentinean (CONICET) research councils, a detailed investigation of the mineralogy of the La Argentina, Nueva Esperanza and La Rosario veins within the Capillitas district was initiated. This study has led to the discovery of at least three new Ge-bearing metallic phases: 1) putzite, this contribution; 2) catamarcaïte (IMA 2003–020),  $\text{Cu}_6\text{GeWS}_8$ , and 3) unnamed  $\text{Cu}_8\text{Fe}_2\text{ZnGe}_2\text{S}_{12}$ , the possible Ge-analogue of stannoidite. Putzite is the most abundant of these.

Putzite is named in honor of Hubert Putz (b. 1973), who discovered the new species during preparation of his Ph.D. thesis on Capillitas, and who identified a significant Ge anomaly in this region. He was also the first to investigate this new species using optical methods and the electron microprobe. The mineral and mineral name have been approved by the Commission of New Minerals and Mineral Names, IMA (2002–024). Holotype material (consisting of two large fragments and one polished section) is deposited under catalogue numbers

14835–14837 in the systematic mineral collection of the Division of Mineralogy, University of Salzburg, Austria. A powder mount, single-crystal mount and several small fragments of pure material in a plastic container are housed within the Systematic Reference Series of the National Mineral Collection of Canada, Geological Survey of Canada, Ottawa, Ontario, under catalogue number NMCC 68096. A single-crystal mount used for the crystal-structure determination is kept at the Laboratory for Chemical and Mineralogical Crystallography, University of Bern, Switzerland.

#### LOCATION AND GEOLOGY

The Capillitas mining district (lat. 27°21'S, long. 66°23'W), located in the Department of Andalgalá, Catamarca Province, northwestern Argentina, 85 km south of the city of Santa María and 54 km north of the city of Andalgalá, at elevations between 2800 and 3400 m above sea level, is part of the Farallón Negro Volcanic Complex. Detailed studies of the geological evolution and structural geology of the Farallón Negro region were presented by Llambias (1970, 1972), Aceñolaza *et al.* (1982), Sasso (1997) and Sasso & Clark (1998). Márquez-Zavalía (1988, 1999) focussed her work on the mineralogy of the Capillitas deposit. New aspects concerning the geology of the Capillitas district have been described by Breitenmoser (1999) and Hug (1999).

The Farallón Negro Volcanic Complex (Fig. 1A) consists of Miocene extrusive rocks, as well as intrusive subvolcanic rocks of largely andesitic composition, and covers an area of approximately 700 km<sup>2</sup>. Intrusive rocks range from andesitic to dacitic to rhyolitic in composition, are restricted to various volcanic centers (Fig. 1A), and host porphyry Cu–Au deposits (*e.g.*, Bajo de la Alumbraera, Agua Rica) and epithermal vein-type deposits (Farallón Negro – Alto de la Blenda, Capillitas). These volcanic rocks overlie Tertiary continental red beds of the El Morterito Formation. The underlying crystalline basement consists of metapelites and schists of the lower Cambrian Suncho Formation and the upper Ordovician to lower Silurian Capillitas granitic batholith.

The Capillitas diatreme cuts the granitic basement block of the Sierra de Capillitas (Figs. 1A, B). The diatreme is composed of intrusive and volcanoclastic rocks (ignimbrite, rhyolite porphyry, dacite porphyry and tuffs) of Miocene age (~5 Ma). Basaltic, melanocratic and rhyolitic dykes are exposed north and west of the diatreme. During a late-stage geological event, hydrothermal fluids altered the diatreme volcanic rocks and produced a series of epithermal polymetallic veins in and around the diatreme. It is host to a subvolcanic, polymetallic, epithermal vein-type deposit, which contains the world's largest gem-type rhodochrosite mineralization (Márquez-Zavalía 1988, 1999). Both the dykes and polymetallic veins follow the two main joint sys-

tems (ENE–WSW and WNW–ESE) in the Capillitas granite.

#### MINERALIZATION

The epithermal veins are hosted in rhyolite, ignimbrite and granite north and west of the Capillitas diatreme (Fig. 1B), and are associated with silicification, and advanced argillic and sericitic alteration. Two preferred orientations are observed: ENE–WSW (*e.g.*, La Rosario, La Grande, La Argentina, Nueva Esperanza and Luisita veins) and WNW–ESE (*e.g.*, Capillitas, Nueve, Ortiz, Restauradora and Bordon veins). These major mineralized veins consist of many smaller veins and veinlets that pinch, swell and anastomose. The average thickness is 50–70 cm, and they extend laterally from 100 to 800 m (Márquez-Zavalía 1988, 1999). Open-space filling, rhythmic banding and brecciation are common textures. At the surface, the mineralized veins are only observable in the Capillitas granite, where they form silicified outcrops of brown to black color owing to oxidation of sulfides and rhodochrosite. Several stages of mineralization were identified (Márquez-Zavalía 1988, 1999); these show a complex Cu–Pb–Zn–Fe–As–Sb–Au–Ag paragenesis, with Bi, W, Sn, Te, Ge, Cd, In, V, Ni, Co and Tl in traces. Quartz, rhodochrosite, barite and alunite are the associated gangue minerals.

The different geological environments, the alteration features, and the ore mineralogy enable us to distinguish between low- and high-sulfidation environments. The high-sulfidation assemblages are composed of pyrite, enargite, tennantite–goldfieldite, hübnerite, sulfosalts of Bi, sulfides of Sn, ± native gold in a quartz–alunite gangue, and are mainly restricted to the diatreme volcanic rocks. The veins hosted in granite remote from the diatreme show typical low-sulfidation assemblages with galena, Fe-poor sphalerite, chalcocopyrite, pyrite, marcasite, ± native silver and sulfides of Ag, with rhodochrosite, quartz and barite as predominant gangue minerals. This latter type of mineralization is also found in the diatreme-hosted veins, but is distinctly separated by brecciation from the older high-sulfidation mineralization.

A significantly different assemblage of minerals is represented by bornite–digenite–chalcocite-rich ores that are restricted to old dumps near the Rosario vein (Fig. 1B). This assemblage is typified by a very complex mineralogy, and several subtypes can be recognized. Massive bornite – digenite – chalcocite ore with subordinate pyrite, tennantite, wittichenite, sphalerite, mawsonite and thalcosite yielded two new Ge-bearing phases [putzite and unnamed Cu<sub>8</sub>Fe<sub>2</sub>ZnGe<sub>2</sub>S<sub>12</sub> (Putz *et al.* 2002a)]. Hübnerite-rich samples of this massive ore contain catamarcaite, ideally Cu<sub>6</sub>GeWS<sub>8</sub>, which has been recently approved by the CNMMN, IMA (2003–020) (Putz *et al.* 2002a). A more stockwork-like sub-

type is characterized by the abundant deposition of Sn-bearing (mawsonite, colusite–nekrasovite, stannoidite) and Te-bearing minerals (goldfieldite, hessite).

#### APPEARANCE AND PHYSICAL PROPERTIES

Putzite is a rare species at Capillitas, and only two putzite-bearing specimens have been collected. They were discovered in old dumps near the Rosario shaft, which is at (WGS 84) 27°20'27" S (latitude), 66°23'21"

W (longitude) and at an altitude of 3240 m above sea level. Putzite is associated with vuggy bornite–chalcocite ore, where it is found embedded as anhedral grains and aggregates, which may attain a size up to  $3 \times 1$  mm. The amount of putzite varies in the two samples. In sample 1, which is considered the holotype and measures  $10 \times 8 \times 8$  cm, the new phase is concentrated in a few  $\text{cm}^3$  of the specimen and is associated with minor catamarcaite, "Ge-stannoidite" (unnamed  $\text{Cu}_8\text{Fe}_2\text{ZnGe}_2\text{S}_{12}$ ), sphalerite, wittichenite, tennantite

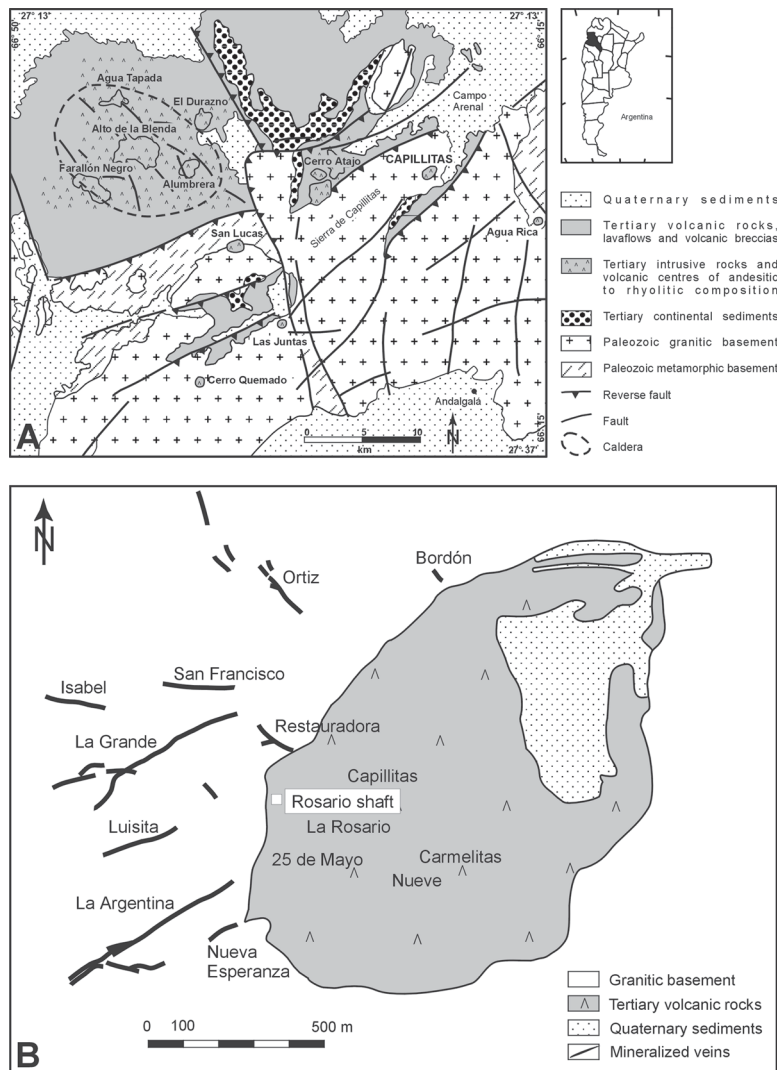


Fig. 1. A) Simplified geological map of the Farallón Negro – Capillitas region, Catamarca Province, Argentina (modified after Breitenmoser 1999). B) Simplified geological map of the Capillitas deposit (modified after Márquez-Zavala 1988) and location of ore veins.

and thalcosite (Figs. 2A, B). The occurrence of thalcosite, which forms tabular grains up to  $260 \times 35 \mu\text{m}$ , is the first report of this mineral in an epithermal deposit (Putz *et al.* 2002b). In sample 2, which measures  $4 \times 3 \times 2 \text{ cm}$ , putzite is present only in minor quantities (Figs. 2C, D). The major Ge-bearing phase in this specimen is catamarcaite, which also is associated with hübnerite, minor “Ge-stannoidite” (unnamed

$\text{Cu}_8\text{Fe}_2\text{ZnGe}_2\text{S}_{12}$ ), luzonite and sphalerite. Thalcosite is not present in sample 2.

Putzite is iron-black with a weak violet tint, which is more pronounced in polished sections (Fig. 2); it has a metallic luster, a black streak, and is opaque. The distinctly brittle mineral has an irregular to subconchoidal, rarely splintery, fracture. Neither cleavage nor parting is obvious in hand specimens. In polished sections, how-

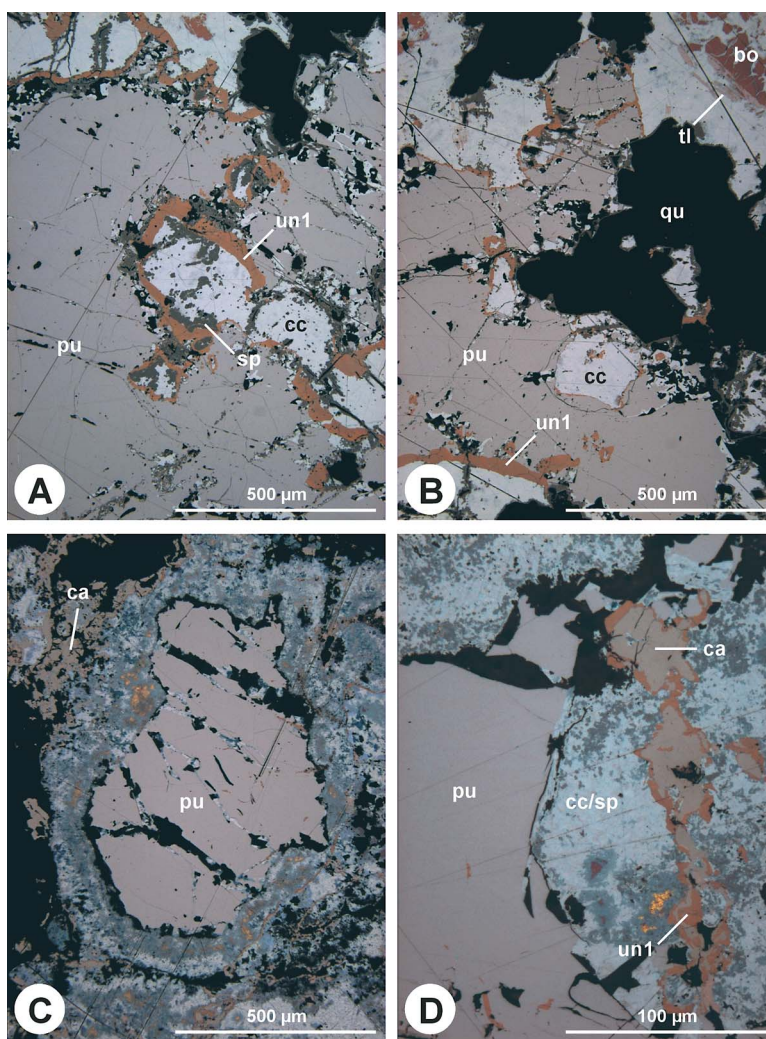


FIG. 2. A) Putzite (pu) rimmed by unnamed  $\text{Cu}_8\text{Fe}_2\text{ZnGe}_2\text{S}_{12}$  (un1) in association with chalcocite (cc) and sphalerite (sp) (sample PR/C2). B) Putzite (pu) rimmed by unnamed  $\text{Cu}_8\text{Fe}_2\text{ZnGe}_2\text{S}_{12}$  (un1) in association with thalcosite (tl), bornite (bo), chalcocite (cc), sphalerite and quartz (qu) (sample PR/C2). C) Relic of putzite (pu) in a fine-grained chalcocite – sphalerite – chalcopyrite – covellite matrix associated with catamarcaite (ca) (sample X19/P2). D) Putzite (pu) in close association with unnamed  $\text{Cu}_8\text{Fe}_2\text{ZnGe}_2\text{S}_{12}$  (un1) and catamarcaite (ca), as inclusions in chalcocite–sphalerite (cc/sp) (sample X19/P2).

ever, a distinct cleavage along an unknown direction can be observed (Figs. 2A, C).

The density, calculated on the basis of the empirical formula, is 5.788 g/cm<sup>3</sup>, a value distinctly lower than that of argyrodite, Ag<sub>8</sub>GeS<sub>6</sub> ( $D_{\text{meas}}$  6.2,  $D_{\text{calc}}$  5.98 g/cm<sup>3</sup>). The Mohs hardness is 3–3½ because calcite is easily scratched, whereas fluorite is not. Microhardness measurements were performed with a Miniload 2 hardness tester using a load of 50 g. The Vickers hardness ranges between 183 and 201, mean 188 km/mm<sup>2</sup>. The calculated Mohs hardness is ≥3 using the equation of Young & Millman (1964) and is in good agreement with the measured Mohs hardness.

#### OPTICAL PROPERTIES

Several fragments of putzite-bearing ore were prepared for optical investigation using the Rehwald technique. This technique involves diamond polishing on laps composed of lead–antimony and lead–tin alloys, which results in almost relief-free polished surfaces (Mücke 1989).

In plane-polarized reflected light (~3200 K), putzite has a pale rose to pale violet color, which is very distinct compared to the associated chalcocite, and is considerably enhanced in oil. Putzite is optically isotropic and does not have internal reflections. It is not light-sensitive, which is in strong contrast with argyrodite. Reflectance measurements were made within the visible spectrum (400–700 nm) at intervals of 20 nm using a Leitz MPV–SP microscope-spectrophotometer (Table 1, Fig. 3). A WTiC reflectance standard (Zeiss 314) was used as a reference for the air and oil ( $N_D = 1.518$ ) measurements. These measurements were

TABLE 1. REFLECTANCE DATA FOR PUTZITE AND ARGYRODITE

$\lambda$ (nm)	Putzite		Argyrodite (Bolivia)			
	$R$ , %	$^{im}R$ , %	$R_1$ , %	$R_2$ , %	$^{im}R_1$ , %	$^{im}R_2$ , %
400	33.5	16.6	27.4	29.3	11.1	12.0
420	31.6	15.2	26.0	27.6	10.7	11.6
440	30.6	14.5	25.2	26.6	10.3	11.0
460	29.4	13.9	24.5	25.9	9.9	10.6
470	28.9	13.5	24.2	25.6	9.8	10.5
480	28.6	13.1	24.0	25.2	9.7	10.4
500	27.8	12.6	23.7	24.8	9.7	10.3
520	27.2	12.1	23.5	24.5	9.6	10.2
540	26.7	11.7	23.3	24.3	9.5	10.0
546	26.5	11.6	23.3	24.2	9.4	10.0
560	26.3	11.5	23.3	24.2	9.4	10.0
580	26.0	11.2	23.2	24.2	9.4	10.0
589	25.8	11.1	23.2	24.1	9.4	10.0
600	25.7	11.0	23.1	24.0	9.5	10.0
620	25.4	11.0	23.1	24.0	9.5	10.0
640	25.3	10.9	23.1	23.9	9.5	10.0
650	25.3	10.9	23.2	24.0	9.5	10.0
660	25.2	10.9	23.2	24.0	9.6	10.1
680	25.2	10.9	23.2	24.0	9.6	10.1
700	25.2	11.0	23.2	24.1	9.7	10.2

performed with  $\times 20$  objectives, the numerical apertures of which were confined to 0.40, and the diameter of the measured discs was 10  $\mu\text{m}$ .

Under the same conditions, reflectance measurements (in air and in oil) were obtained for argyrodite for comparison (Table 1). The argyrodite sample is from the Hundimiento vein, Porco, Bolivia (Paar 2003) and compositionally corresponds to Ag<sub>8</sub>GeS<sub>6</sub>. The reflectances for argyrodite from Bolivia are slightly lower, and the bireflectances a bit higher, than the values for argyrodite from Freiberg, Saxony, Germany (Criddle & Stanley 1993).

The shape of the reflectance spectra of putzite and Bolivian argyrodite is quite similar, in accordance with the very similar color of both species in reflected light (Fig. 3). From short to long wavelength, a continuous decrease of the reflectance values of putzite is noted, with a slightly sharper decrease in the range between 400 and 500 nm (Fig. 3).

#### CHEMICAL COMPOSITION

Several polished sections containing putzite were prepared from the two specimens and analyzed with a JEOL Superprobe JXA–8600, controlled by an ELX

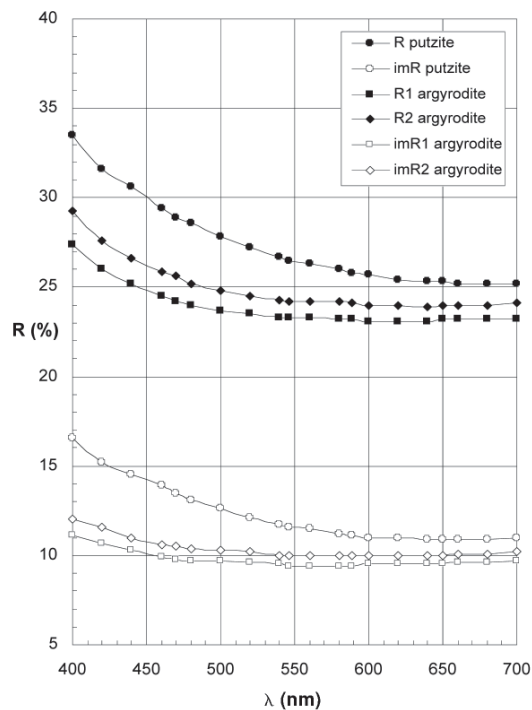


FIG. 3. Reflectance spectra, in air and in immersion oil, for putzite ( $R$ ,  $^{im}R$ ) and argyrodite ( $R_1$ ,  $R_2$ ,  $^{im}R_1$ ,  $^{im}R_2$ ).

system, and utilizing an operating voltage of 25 kV and a beam current of 10 nA.

The polished surface of putzite is sensitive to electron-beam interaction; in order to carry out reliable quantitative analyses, the diameter of the beam was defocused to  $\sim 10 \mu\text{m}$  and the stage moved during measurements. Chalcopyrite ( $\text{CuFeS}_2$ ;  $\text{CuK}\alpha$ ), stephanite ( $\text{Ag}_5\text{SbS}_4$ ;  $\text{AgL}\alpha$ ,  $\text{SK}\alpha$ ) and Ge metal ( $\text{GeK}\alpha$ ) were used as standards. Zn, Fe, Cd, Sn and As were sought, but not detected. The raw data were processed with the on-line ZAF-4 program.

The results, obtained from five grains in two different polished sections, show only minor variation of the chemical composition (Table 2). The average result of 29 point analyses of four grains from sample 1 (PR/C2) is: Cu 33.04, Ag 39.33, Ge 7.79, S 20.55, total 100.71 wt.%, corresponding to  $(\text{Cu}_{4.78}\text{Ag}_{3.35})_{\Sigma 8.13}\text{Ge}_{0.99}\text{S}_{5.89}$  (on the basis of total atoms = 15). If the formula is recalculated for Cu + Ag = 8 with Cu/Ag = 1.43 (Table 2), the composition is  $(\text{Cu}_{4.71}\text{Ag}_{3.29})_{\Sigma 8}\text{GeS}_6$  or, ideally,  $(\text{Cu}_{4.7}\text{Ag}_{3.3})_{\Sigma 8}\text{GeS}_6$ . The ideal formula requires: Cu 32.48, Ag 38.71, Ge 7.89, S 20.92, total 100.00 wt.%. The average result of six point-analyses of sample 2 (X19/H8) is: Cu 32.71, Ag 39.83, Ge 7.62, S 20.59, total 100.75 wt.%, corresponding to  $(\text{Cu}_{4.73}\text{Ag}_{3.40})_{\Sigma 8.13}\text{Ge}_{0.97}\text{S}_{5.91}$  (on the basis of total atoms = 15). The Cu:Ag ratio is 1.39, which is slightly lower than for sample 1. The excess of Ag in several compositions listed in Table 2 is interpreted as an analytical artifact due to beam-sensitivity issues.

TABLE 2. THE COMPOSITION OF PUTZITE FROM ITS TYPE LOCALITY, CAPILLITAS MINING DISTRICT, CAMARCA, ARGENTINA

Sample		Cu	Ag	Ge	S	Total
PR/C2-gr1	<i>n</i> = 7 mean	33.20	39.19	7.81	20.68	100.88
	s.d. <sup>1</sup>	0.22	0.46	0.11	0.26	0.23
PR/C2-gr1a	<i>n</i> = 10 mean	33.16	39.27	7.79	20.52	100.75
	s.d.	0.32	0.73	0.11	0.23	0.43
PR/C2-gr2	<i>n</i> = 4 mean	32.58	39.88	7.76	20.36	100.58
	s.d.	0.37	0.46	0.06	0.26	0.32
PR/C2-gr2a	<i>n</i> = 8 mean	32.96	39.23	7.79	20.58	100.56
	s.d.	0.34	0.72	0.11	0.23	0.49
PR/C2 ave.	<i>n</i> = 29 mean	33.04	39.33	7.79	20.55	100.71
	s.d.	0.36	0.65	0.10	0.25	0.40
	min	32.26	38.14	7.59	20.14	100.50
	max	33.60	40.54	8.00	20.95	101.50
X19/H8	<i>n</i> = 6 mean	32.71	39.83	7.62	20.59	100.75
	s.d.	0.27	0.32	0.11	0.12	0.38
	min	32.41	39.36	7.42	20.42	100.27
	max	33.09	40.31	7.73	20.70	101.19
<b>formula (<math>\Sigma\text{M} + \text{S} = 15 \text{ apfu}</math>)</b>						
		Cu	Ag	Ge	S	Cu+Ag Cu/Ag <sup>2</sup>
PR/C2-gr1		4.78	3.33	0.98	5.91	8.11 1.44
PR/C2-gr1a		4.79	3.34	0.99	5.88	8.13 1.43
PR/C2-gr2		4.74	3.41	0.99	5.86	8.15 1.39
PR/C2-gr2a		4.77	3.34	0.99	5.90	8.11 1.43
PR/C2 average		4.78	3.35	0.99	5.89	8.13 1.43
X19/H8		4.73	3.40	0.97	5.91	8.13 1.39

<sup>1</sup> Standard deviation. <sup>2</sup> Ratio of atoms.

## X-RAY CRYSTALLOGRAPHY

A fragment of putzite, about 0.2 mm in longest dimension, from a crushed crystalline aggregate, was studied by single-crystal precession methods employing Zr-filtered Mo radiation. The fragment was mounted such that  $a^*$  is parallel to the dial axis; the following levels were collected:  $hk0$ ,  $hkl$  and  $a^* \wedge 011^*$ . Precession films indicate a cubic symmetry, with a measured unit-cell parameter  $a$  equal to 10.195 Å. Systematic absences dictate a  $F$ -centered lattice with the following permissible space-groups:  $Fm\bar{3}m$  (225),  $F432$  (209) or  $F\bar{4}3m$  (216). The diffraction symmetry is  $m\bar{3}m$  (as opposed to  $m\bar{3}$ , which excludes space groups  $Fm\bar{3}$  and  $F23$ ). The refined unit-cell parameter  $a$  10.201(3) Å,  $V$  1061.5(6) Å<sup>3</sup>, is based on the  $d$  values of 11 X-ray powder lines between 3.076 and 1.538 Å for which unambiguous indexing was possible, based on visual inspection of single-crystal precession films. All possible reflections down to 1.41 Å were visually examined on single-crystal precession films. A fully indexed X-ray powder pattern obtained with a 114.6 mm Debye-Scherrer camera is presented in Table 3.

A black and platy fragment of putzite, displaying the shape of an irregular pentagon and about  $0.15 \times 0.12 \times 0.03$  mm in size, was measured on an ENRAF NONIUS CAD4 single-crystal X-ray diffractometer using graphite monochromated  $\text{MoK}\alpha$  X-radiation. The cell parameter was refined from 24 sharp reflections with high  $\theta$  angles and yielded cubic symmetry and the cell parameter listed in Table 4. There were no indications that cubic symmetry is an artifact due to twinning of low-symmetry individuals. Experimental details are given in Table 5. Diffraction data were collected up to  $\theta = 30^\circ$  and data reduction, including background and Lorentz polarization correction, was carried out with the SDP program system (ENRAF NONIUS 1983). An empirical absorption correction using the  $\Psi$ -scan technique was routinely applied. From the various space-groups proposed by the program XPREP (Bruker AXS 1997),

TABLE 3. X-RAY POWDER-DIFFRACTION DATA FOR PUTZITE

I est	<i>d</i> meas	<i>d</i> calc	<i>hkl</i>	I est	<i>d</i> meas	<i>d</i> calc	<i>hkl</i>
30	5.896	5.890	111	* 70	1.805	1.803	440
* 60	3.074	3.076	311	* 25	1.725	1.724	531
* 100	2.943	2.945	222	* 15	1.701	1.700	600
5	2.557	2.550	400				442
* 20	2.343	2.340	331	* 10	1.610	1.613	620
5	2.283	2.281	420	* 10	1.558	1.556	533
* 30	2.083	2.082	422	* 15	1.534	1.538	622
			333				
* 50	1.962	1.963	511				

114.6 mm Debye-Scherrer powder camera; Cu radiation, Ni-filter ( $\lambda$   $\text{CuK}\alpha = 1.54178$  Å). The intensities were estimated visually. The pattern was not corrected for shrinkage, and no internal standard was added. \* Reflection used for unit-cell refinement. The pattern was indexed on  $a$  10.201 Å.

$F\bar{4}3m$  (216), the one with the highest possible symmetry, was used for the structure solution and refinement. As will be shown below, putzite is an argyrodite-group mineral. Space groups in this group of minerals and related synthetic compounds may be orthorhombic (*e.g.*,  $\text{Cu}_8\text{GeS}_6$  and  $\text{Ag}_8\text{GeS}_6$ ) and in disordered examples, also up to cubic. There are characteristic subgroup – supergroup relationships among the observed space-groups (Unterrichter von Reichtenthal & Range 1978), which predict  $F\bar{4}3m$  for the cubic case. One of the characteristic structural features of argyrodite-group compounds is the occurrence of so-called supertetrahedra, which (in cubic symmetry) can only realized by a  $\bar{4}$  operation. For this reason, other space groups (without  $\bar{4}$ ), permissible on the basis of systematic absences, could be rejected. Nevertheless, before the argyrodite-type structure of putzite was verified, we also tested the other space groups in the structure solution, but without success.

#### STRUCTURE DETERMINATION AND REFINEMENT

The structure was solved by direct methods (program SHELXS; Sheldrick 1997a) that revealed the Ge atom and some additional positions. In subsequent cycles of refinement (program SHELXL; Sheldrick 1997b), the remaining atom-positions were deduced from the difference-Fourier syntheses by selecting from among the strongest maxima at appropriate distances. Cation assignment was guided by knowledge of the chemical composition of the crystal. The final refinement was performed with anisotropic-displacement parameters for all positions except *M2* and an empirical extinction-coefficient. To reduce the number of least-squares parameters and the correlations with  $U_{ij}$ , the site-occupancy factors were fixed for the last cycles of refinement (fully occupied: Cu1 and Ag1; partly occupied: *M2*). The Cu,Ag populations at site *M2* were chosen (and fixed) in a way that the refined formula of putzite corresponds to one of the chemical compositions. The highest residual peak was  $1.71 \text{ e}/\text{\AA}^3$ ,  $1.20 \text{ \AA}$  from Ag1, and the deepest hole was  $-1.11 \text{ e}/\text{\AA}^3$ ,  $1.01 \text{ \AA}$  from S1 at the end

TABLE 4. UNIT-CELL DATA OF PUTZITE AND SELECTED SYNTHETIC COMPOUNDS OF THE ARGYRODITE GROUP

	Putzite	Synthetic	Synthetic	Synthetic
Formula	$\text{Cu}_4\text{Ag}_{3.1}\text{GeS}_6$	$\text{Cu}_8\text{GeS}_6$	$\text{Ag}_8\text{GeS}_6$	$\text{Ag}_8\text{GeS}_6$
System	cubic	orthorhombic	orthorhombic	orthorhombic
Space group	$F\bar{4}3m$	$Pmn2_1$	$Pna2_1$	$Pna2_1$ , or $Pnam$
<i>a</i> (Å)	10.1250(12)	7.0445(3)	15.149(1)	15.133(2)
<i>b</i> (Å)		6.9661(1)	7.476(2)	7.463(1)
<i>c</i> (Å)		9.8699(5)	10.589(1)	10.583(2)
<i>V</i> (Å <sup>3</sup> )	1037.97	484.3	1199.2	1195.2
<i>Z</i>	4	2	4	4
Reference	This study	Ishii <i>et al.</i> (1999)	Eulenberger (1977)	Wang (1978)

of the refinement. The refinement was stopped when the mean shift/esd for various parameters dropped below 1%. It indicates close metal–metal contacts, which indicate Cu,Ag disorder. Twinning by the inversion operation was not observed. Fractional coordinates and equivalent-isotropic displacement parameters of atoms in putzite are listed in Table 6. Anisotropic-displacement parameters are listed in Table 7. Selected interatomic distances are given in Table 8. Observed and calculated structure-factors are available from The Depository of Unpublished Data, CISTI, National Research Council, Ottawa, Ontario K1A 0S2, Canada.

#### THE CRYSTAL STRUCTURE OF PUTZITE

The crystal structure of putzite is rather complex and difficult to present properly in projection. The description of the structure follows previously published results

TABLE 5. DATA COLLECTION AND REFINEMENT PARAMETERS FOR PUTZITE

Diffractometer	ENRAF NONIUS CAD4
X-ray radiation	fine-focus sealed tube, MoK $\alpha$
X-ray power	50 kV, 40 mA
Temperature	293 K
Maximum $2\theta$	60.17°
Resolution (approximate)	0.7 Å
Measured reflections	259
Index range	$0 \leq h \leq 10, 0 \leq k \leq 14, 0 \leq l \leq 14$
Observed reflections	259
Unique reflections	110
Reflections $> 2\sigma(I)$	90
$R_{\text{INT}}$	5.97%
$R_{\sigma}$	5.25%
Number of least-squares parameters	23
Goof	1.211
$R_1, F_o > 4 \sigma(F_o)$	5.62%
$R_1$ , all data	6.82%
$wR_2$ (on $F_o^2$ )	16.93%
$R_{\text{INT}} = \Sigma  F_o^2 - F_c^2(\text{mean})  / \Sigma F_o^2$	$R_{\sigma} = \Sigma \sigma(F_o^2) / \Sigma F_o^2$
$R_1 = \Sigma   F_o  -  F_c   / \Sigma  F_o $	$wR_2 = \{(\Sigma w[F_o^2 - F_c^2]^2) / \Sigma w[F_o^2]^2\}^{1/2}$
$\text{Goof} = \{(\Sigma w[F_o^2 - F_c^2]) / [n-p]\}^{1/2}$	$w = 1 / (\sigma^2[F_o^2] + [0.1171 P]^2 + [5.92 P])$
$P = (\max(F_o^2, 0) + 2 F_c^2) / 3$	

TABLE 6. LABELS, OCCUPANCY FACTORS, FRACTIONAL COORDINATES, AND EQUIVALENT ISOTROPIC DISPLACEMENT-PARAMETERS OF ATOMS IN PUTZITE

Atom	sof <sup>1)</sup>	<i>x/a</i>	<i>y/b</i>	<i>z/c</i>	$U_{\text{iso}}$
Ge1	1	0	0.5	0	0.0127(13)
Cu1	0.5	0.25	0.75	0.9804(8)	0.059(3)
Ag1	0.25	0.3279(9)	0.4713(13)	0.1721(9)	0.072(4)
Cu2 <sup>2)</sup>	0.14	0.355(3)	0.564(4)	0.145(3)	0.118(12) <sup>3)</sup>
Ag2 <sup>2)</sup>	0.04	0.355(3)	0.564(4)	0.145(3)	0.118(12) <sup>3)</sup>
S1	1	0.1250(3)	0.6250(3)	0.1250(3)	0.0208(16)
S2	1	0.25	0.75	0.75	0.051(5)
S3	0.25	0.5206(11)	0.5206(11)	0.0206(11)	0.023(8)

<sup>1)</sup> site-occupancy factor; formula derived:  $\text{Cu}_{4.7}\text{Ag}_{5.3}\text{GeS}_6$

<sup>2)</sup> denoted *M2* in the text

<sup>3)</sup> refined only isotropically

of argyrodite structures *sensu lato* only in the case of the  $MS_4$  tetrahedra. Instead of discussing various two-, three-, or four-fold coordinations around (disordered) Ag and Cu, the very regular metal coordinations around the S2 and S3 atoms are discussed, and the structure successively built up by defining adequate and simple polyhedra. However, these simple polyhedra remain, to a certain extent, a tool to illustrate the structure, but do not exist in reality because close metal-metal contacts make their existence impossible.

Based upon a scheme of closest packing, S1 atoms build up an open framework of filled and empty tetrahedra, respectively. This same framework can be defined in the (orthorhombic) crystal structure of synthetic  $Cu_8GeS_6$  (Ishii *et al.* 1999, Onoda *et al.* 1999). Four  $GeS(1)_4$  tetrahedra are arranged in the form of a supertetrahedron (Fig. 4A). Similar supertetrahedra occur in synthetic  $Cu_8GeS_6$  (Ishii *et al.* 1999, Onoda *et al.* 1999). In this supertetrahedron, the  $GeS(1)_4$  tetrahedra are interconnected *via* S1–Cu1–S1 (or S1–Ag2–S1 or S1–M2–S1) bonds (Fig. 4B). S2, in the center of the supertetrahedron, and six surrounding Cu1 form regular  $SCu_6$  octahedra (Fig. 4C). In synthetic  $Cu_8GeS_6$  (Ishii *et al.* 1999, Onoda *et al.* 1999), these octahedra are very distorted and would be better described as distorted “square” pyramids with an additional distant ligand that completes the “octahedral” environment. Ag is displaced from the above Cu position; the Cu–Ag separation is 1.119(11) Å, and the Ag–Ag distance (along Ag–Cu–Ag) is 2.231(13) Å (Table 8). If S2 bonds to Ag instead of Cu, the resulting coordination polyhedron is a (dominant) tetrahedron {111} with all apices cut off by an inverted tetrahedron  $\{\bar{1}\bar{1}\bar{1}\}$  (Fig. 4D). Obviously, this kind of polyhedron does not exist in reality because not all Ag positions with partial occupancy can be occupied locally owing to the short Ag–Ag contacts that would result. As mentioned above, S1 from the  $GeS_4$  tetrahedra can also be interconnected *via* M2. The S1–M2 distance of 2.418(31) Å is intermediate between the S1–Cu1 and the S1–Ag1 bond lengths of 2.312(6) and 2.621(11) Å, respectively. However, S2 does not form bonds with M2 because the shortest S2–M2 distance is 3.517(31) Å.

Four supertetrahedra occur per unit cell (Fig. 4E). They interpenetrate in such a way that they all share the common  $GeS(1)_4$  tetrahedron centered around  $\frac{1}{2} \frac{1}{2} \frac{1}{2}$ , as shown in Figure 4F. A similar arrangement is ob-

served in synthetic  $Cu_8GeS_6$  (Ishii *et al.* 1999, Onoda *et al.* 1999). This arrangement of supertetrahedra hosts cavities (see below) centered around special position 0,0,0. Atom S3 is located close to this special position, forming a tiny  $S(3)_4$  tetrahedron (simplified as spheres in Figs. 4g, h). If S3 is only surrounded by Cu1, a regular cuboctahedron results (Fig. 4G). If S3 is surrounded by Ag1 or M2, irregular cuboctahedra result (not shown). These arrangements give rise to many possible bond formations between S3 and either M2 or Ag1 at appropriate distances. Cu1 is very distant from S3 and, therefore, no S3–Cu1 bonds can be formed (the shortest S3–Cu1 distance is 3.285 Å). The above mentioned (regular or irregular) cuboctahedra complete the three-dimensional framework of putzite (Fig. 4B). In synthetic  $Cu_8GeS_6$  (Ishii *et al.* 1999, Onoda *et al.* 1999), these interstices are occupied by “square” pyramids with rectangular bases. These regular (and irregular) polyhedra and their mutual arrangements help to illustrate the average structure of putzite. It is evident that such polyhedra, with only one type of ligand (*e.g.*,  $SCu_6$ ,  $SAg_{12}$ ,  $SM_{12}$ ), do not and cannot exist in reality for various reasons, but only cations forming bonds with two, three or four S atoms.

#### BOND-LENGTH ANALYSIS AND CU, AG ORDER-DISORDER

The  $GeS_4$  tetrahedra have four Ge1–S1 bonds of 2.192(3) Å (Table 8), which correspond well to the mean Ge–S distance of 2.212 Å (range: 2.200–2.227 Å) found for the synthetic low-temperature modification of argyrodite (Eulenberger 1977). The  $GeS_4$  tetrahedra can be interconnected either *via* S–Cu–S, S–Ag–S, or S–M–S bonds, as discussed above. In all cases, reasonable bond-distances result (Table 8): the Cu–S1 bonds are 2.312(6) Å, and the Cu–S2 bond is 2.333(8) Å, both significantly shorter than the Ag–S1 bond, 2.621(11) Å, and the Ag–S2 bond, 2.503(12) Å. For synthetic  $Cu_8GeS_6$ , Ishii *et al.* (1999) listed Cu–S bonds in the

TABLE 8. SELECTED INTERATOMIC DISTANCES FOR PUTZITE

Central atom	Ligand	Polyhedron	Bonds	Distances (Å)	
Ge1	S1	$GeS_4$ tetrahedron	Ge–S	2.192(3)	4×
S2	Cu1	$SCu_6$ octahedron	S–Cu	2.333(8)	6×
S2	Ag1	$SAg_{12}$ two combined tetrahedra	S–Ag	2.503(10)	12×
S2	M2	$SM_{12}$ two combined tetrahedra	S–M	3.517(31)	12×
S3	M2	$SM_{12}$ cuboctahedron	S–M	1.977(37)	3×
				2.143(39)	6×
				2.521(37)	3×
S3	Ag1	$SAg_{12}$ cuboctahedron	S–Ag	2.171(14)	3×
				2.532(16)	6×
				2.760(16)	3×
S3	Cu1	$SCu_{12}$ cuboctahedron	S–Cu	3.285(13)	3×
				3.615(12)	6×
				3.875(13)	3×

TABLE 7. ANISOTROPIC-DISPLACEMENT PARAMETERS FOR PUTZITE

Site	$U_{11}$	$U_{22}$	$U_{33}$	$U_{23}$	$U_{13}$	$U_{12}$
Ge1	0.0127(13)	0.0127(13)	0.0127(13)	0	0	0
Cu1	0.072(5)	0.072(5)	0.034(5)	0	0	-0.039(7)
Ag1	0.064(4)	0.086(10)	0.064(4)	0.005(4)	-0.021(5)	-0.005(4)
S1	0.0208(16)	0.0208(16)	0.0208(16)	-0.0064(11)	-0.0064(11)	-0.0064(11)
S2	0.051(5)	0.051(5)	0.051(5)	0	0	0
S3	0.023(8)	0.023(8)	0.023(8)	-0.006(4)	-0.006(4)	-0.006(4)

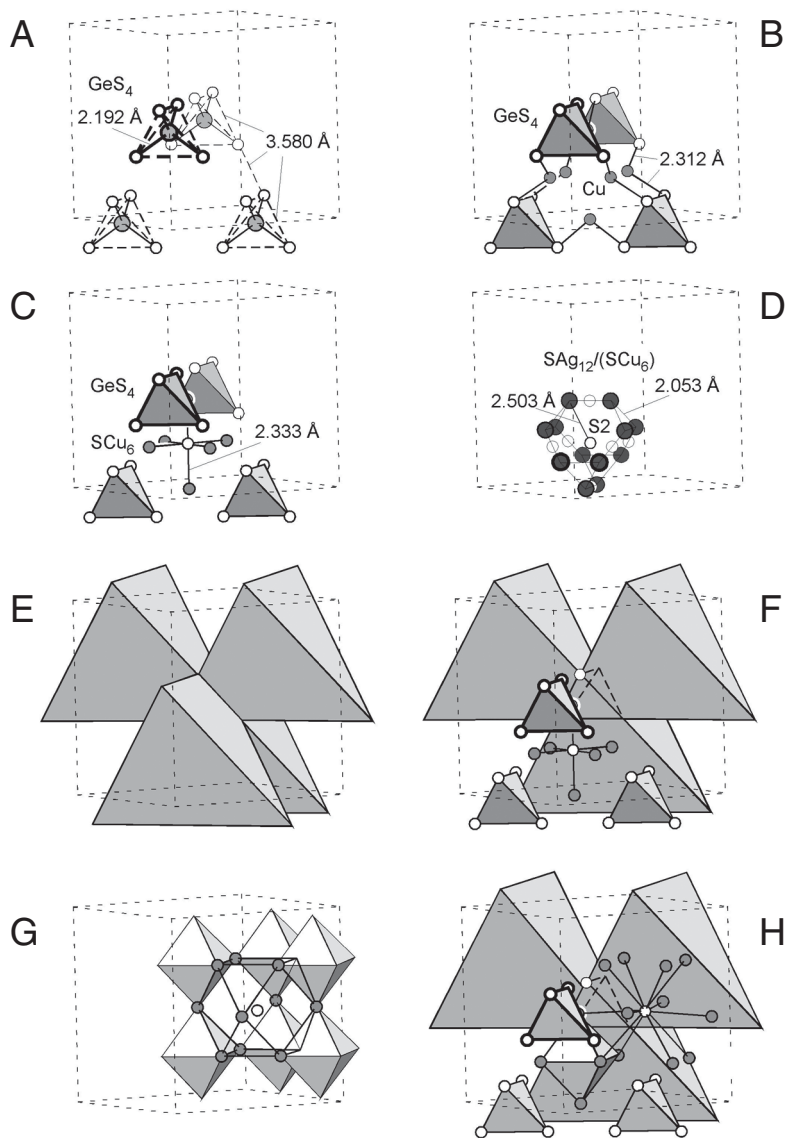


FIG. 4. The crystal structure of putzite: (A)  $\text{Ge}(1)\text{S}(1)_4$  tetrahedra forming a "supertetrahedron"; (B) interconnection of  $\text{GeS}_4$  tetrahedra by  $\text{Cu}(1)\text{--S}(1)$  bonds; (C)  $\text{S}(2)\text{Cu}(1)_6$  octahedron inside the supertetrahedron; (D)  $\text{S}(2)\text{Ag}(1)_{12}$  polyhedron (combination of  $\{111\}$  dominant tetrahedron with  $\{\bar{1}\bar{1}\bar{1}\}$  tetrahedron); (E) arrangement of four supertetrahedra per unit cell; (F) four supertetrahedra sharing a common  $\text{GeS}_4$  tetrahedron at  $\frac{1}{2} \frac{1}{2} \frac{1}{2}$ ; (G) regular  $\text{S}(3)\text{Cu}(1)_{12}$  cuboctahedron; (H) completed structure. See text for details.

range 2.24–2.61 Å. Eulenberger (1977) described Ag–S bond distances in the range 2.416–2.75 Å (for eight different Ag atoms with two, three, or four S ligands). Cu–S and Ag–S bond data for putzite correspond well to the majority of bond distances given by both Ishii *et*

*al.* (1999) and Eulenberger (1977). In Figures 4g and 4h, S3 is, as previously mentioned, ideally shown as a sphere. In fact, four S3 atoms form a small tetrahedron, with the S atoms 0.590(16) Å apart from each other. As can be seen from Table 8, only *M2* and *Ag1* are at ad-

equate bond-forming distances from S3 [2.521(37) and 2.532(16) Å, respectively], whereas Cu1 is too far away [minimum distance 3.285(13) Å] to form a bond.

Putzite is interpreted as a disordered structure in which the coordination polyhedra are statistically occupied in order to avoid short metal–metal bond distances. Although the polyhedra introduced above, with the exception of GeS<sub>4</sub> tetrahedra, do not exist as such, they help enormously to illustrate the putzite structure in a rather simple way.

In general, low-temperature modifications of argyrodite-group compounds are orthorhombic (Table 4), whereas high-temperature modifications may attain cubic symmetry. In case of putzite, with a nonstoichiometric Cu:Ag ratio, we assume that an ordered (low-symmetry) structure could not be realized due to the different bonding requirements of Cu and Ag.

#### RELATIONSHIP TO OTHER MINERALS

Putzite belongs to the argyrodite group of compounds with the general formula  $A^{m+}_{(12-n-y)/m} B^{n+} X^{2-}_{6-y} Y^{-}_y$ , with  $A = \text{Ag}^+, \text{Cu}^+, \text{Cd}^{2+}$ , etc.;  $B = \text{Ga}^{3+}, \text{Si}^{4+}, \text{Ge}^{4+}, \text{Sn}^{4+}, \text{P}^{5+}$ , etc.;  $X = \text{S}, \text{Se}, \text{Te}$ ;  $Y = \text{Cl}, \text{Br}, \text{I}$  (Kuhs *et al.* 1979, Evain *et al.* 1998). They have a common cubic ( $F\bar{4}3m$ ) high-temperature structure ( $\gamma$  phase) with a disordered  $A$ -cation sublattice; at lower temperatures, transitions into various ordered structures ( $\alpha$  and  $\beta$  phases) occur (Kuhs *et al.* 1979, Evain *et al.* 1998). The name of this group of compounds originates from argyrodite, Ag<sub>8</sub>GeS<sub>6</sub>, originally described by Weisbach (1886). Putzite represents the Cu-dominant analogue. Among the various known synthetic members, putzite is only the third known in nature (the other two being argyrodite and canfieldite) and the only one for which single-crystal structure data are available.

Putzite (as chemically analyzed) is an Ag-rich variety of the synthetic inorganic compound  $\gamma$ -Cu<sub>8</sub>GeS<sub>6</sub> [PDF 40–1190; cubic,  $a$  9.926 ; space group  $F\bar{4}3m$  (216),  $Z = 4$ ,  $D$  (calc.) 5.252 g/cm<sup>3</sup>; PSC =  $cF60$ ]. With significant Ag substitution for Cu in the structure, the  $d$  values of the powder pattern, the unit-cell parameter, and the calculated density increase substantially from end-member Cu<sub>8</sub>GeS<sub>6</sub> values. By analogy, the correct space-group for putzite is  $F\bar{4}3m$ , which is one of the space-group choices determined from single-crystal precession studies. Putzite is not directly related to argyrodite *per se*, but is related to the synthetic orthorhombic room-temperature phase of Cu<sub>8</sub>GeS<sub>6</sub> ( $\beta$  phase; Ishii *et al.* 1999, Onoda *et al.* 1999) which, in turn, is related to argyrodite.

#### CONDITIONS OF FORMATION

The concentration of Ge in sulfide deposits, especially those containing Zn–Cu–Pb, is documented from several locations worldwide such as Tsumeb, Namibia

(Söhnge 1964, Geier & Ottemann 1970a, b), Kipushi, Democratic Republic of Congo (Intiomale & Oosterbosch 1974) and Leogang, Salzburg Province, Austria (Paar & Chen 1986). Sulfide ores that formed from solutions with higher activity of sulfur contain Ge in the form of its own sulfides, such as germanite, renierite, briartite or argyrodite (Bernstein 1985). This is also the case at Capillitas, where Ge is present as distinct sulfides (putzite, catamarcaite, unnamed Cu<sub>8</sub>Fe<sub>2</sub>ZnGe<sub>2</sub>S<sub>12</sub>).

On the basis of textural evidence, the formation of putzite and the other commonly intergrown Ge-bearing sulfides represents an early stage in the crystallization sequence. Chalcocite, which contains relics of bornite, tennantite, wittichenite, thalcosite and other minor phases (mawsonite, galena), is a late phase and is possibly indicative of secondary (supergene) replacement processes that have led to a significant enrichment in sulfide.

It is not possible, however, to assign a temperature of formation to putzite and the other associated Ge-bearing sulfides. There have been no experimental studies undertaken in the quaternary system Cu–Ag–Ge–S, and the phase relations in the ternary systems Cu–Ge–S (Wang & Viaene 1974, Wang 1988) and Ag–Ge–S (Wang 1978, 1995) are not applicable to the conditions of formation of putzite. The source of the Ge is not known at Capillitas. We speculate that Ge was derived from enrichment processes during the fractional crystallization of fluids derived from an igneous source or is due to the incorporation of Ge from country rocks containing organic matter. The latter source is highly probable at Capillitas because the metamorphic Paleozoic basement rocks commonly contain shales and schists enriched in bituminous material.

#### ACKNOWLEDGEMENTS

WHP expresses his thanks to the Austrian Science Foundation (FWF) which supported, through grants P 11987 and 13974, field and laboratory work in both Argentina and Austria. We thank Prof. Ricardo Sureda (University of Salta, Argentina) for logistical help during field work in Argentina, Hubert Putz (University of Salzburg) for providing the specimens for study purposes, and Winfried Waldhör (University of Salzburg) for the preparation of polished sections. Margit Ebner (University of Salzburg) patiently typed various drafts of the manuscript. Finally, we acknowledge the comments of Robert R. Seal II, Joseph A. Mandarino, Joel D. Grice, an anonymous referee, and Robert T. Downs, which contributed to improve the paper.

#### REFERENCES

- ACEÑOLAZA, F.G., TOSELLI, A.J., DURAND, F.R. & DÍAZ TADEI, R. (1982): Geología y estructura de la región norte de Andalgalá, Provincia de Catamarca. *Acta Geológica Lilloana* **16**, 121–139.

- BERNSTEIN, L.R. (1985): Germanium geochemistry and mineralogy. *Geochim. Cosmochim. Acta* **49**, 2409-2422.
- BREITENMOSER, T. (1999): *Geology and Geochemistry of the Calc-Alkaline Farallón Negro Volcanic Complex at Capillitas, NW-Argentina*. M.Sc. thesis, ETH, Zürich, Switzerland.
- BRUKER AXS (1997): XPREP Ver. 5.1: A computer program for data preparation and reciprocal space exploration. Bruker Analytical X-ray systems, Madison, Wisconsin 53719-1173, USA.
- CRIDDLE, A.J. & STANLEY, C.J. (1993): *The Quantitative Data File for Ore Minerals*. The Commission on Ore Mineralogy, International Mineralogical Association. Chapman & Hall, London, U.K.
- ENRAF NONIUS (1983): Structure determination package (SDP). Enraf Nonius, Delft, The Netherlands.
- EULENBERGER, G. (1977): Die Kristallstruktur der Tieftemperaturmodifikation von  $\text{Ag}_8\text{GeS}_6$ , synthetischer Argyrodit. *Monatsh. Chem.* **108**, 901-913.
- EVAIN, M., GAUDIN, E., BOUCHER, F., PETŘÍČEK, V. & TAULELLE, F. (1998): Structures and phase transitions of the  $\text{A}_7\text{PSe}_6$  (A = Ag, Cu) argyrodite-type ionic conductors. I.  $\text{Ag}_7\text{PSe}_6$ . *Acta Crystallogr.* **B54**, 376-383.
- GEIER, B.H. & OTTEMANN, J. (1970a): New primary vanadium, germanium-, gallium-, and tin-minerals from the Pb-Zn-Cu-deposit Tsumeb, South West Africa. *Mineral. Deposita* **5**, 29-40.
- \_\_\_\_\_ & \_\_\_\_\_ (1970b): New secondary tin-germanium and primary tungsten- (molybdenum-, vanadium-) germanium minerals from the Tsumeb ore-deposit. *Neues Jahrb. Mineral., Abh.* **114**, 89-107.
- HUG, A. (1999): *Petrography and Genesis of the Capillitas Diatreme, Farallón Negro Volcanic Complex, NW-Argentina*. M.Sc. thesis, ETH, Zürich, Switzerland.
- INTIOMALE, M.M. & OOSTERBOSCH, R. (1974): Géologie et géochimie de gisement du Kipushi, Zaire. In *Gisements Stratiformes et Provinces Cuprifères* (P. Bartholomé, ed.). Soc. Géol. Belg., Liège, Belgique (123-164).
- ISHII, M., ONODA, M. & SHIBATA, K. (1999): Structure and vibrational spectra of argyrodite family compounds  $\text{Cu}_8\text{SiX}_6$  (X = S, Se) and  $\text{Cu}_8\text{GeS}_6$ . *Solid State Ionics* **121**, 11-18.
- KUHS, W.F., NITSCHKE, R. & SCHEUNEMANN, K. (1979): The argyrodites - a new family of tetrahedrally close-packed structures. *Mater. Res. Bull.* **14**, 241-248.
- LLAMBIÁS, E.J. (1970): Geología de los yacimientos mineros de Agua de Dionisio, Provincia de Catamarca, República Argentina. *Revista Asociación Argentina de Mineralogía, Petrología y Sedimentología* **1**, 2-32.
- \_\_\_\_\_ (1972): Estructura del grupo volcánico Farallón Negro, Catamarca, República Argentina. *Revista Asociación Geológica Argentina* **27**, 161-169.
- MÁRQUEZ-ZAVALÍA, M.F. (1988): *Mineralogía y genesis del yacimiento Capillitas (Catamarca, República Argentina)*. Ph.D. thesis, University of Salta, Salta, Argentina.
- \_\_\_\_\_ (1999): El yacimiento Capillitas, Catamarca. In *Recursos Minerales de la República Argentina* (O. Zappettini, ed.). *Instituto de Geología y Recursos Minerales SEGEMAR, Anales* **35**, 1643-1652.
- MÜCKE, A. (1989): *Anleitung zur Erzmikroskopie mit einer Einführung in die Erzpetrographie*. Ferdinand Enke Verlag, Stuttgart, Germany.
- ONODA, M., CHEN, XUE AN., KATO, K., SATO, A. & WADA, H. (1999): Structure refinement of  $\text{Cu}_8\text{GeS}_6$  using X-ray diffraction data from a multiple-twinning crystal. *Acta Crystallogr.* **B55**, 721-725.
- PAAR, W.H. (2003): La presencia y distribución del germanio e indio en la mena del yacimiento Zn-Pb-Ag Porco, Departamento Potosí, Bolivia. Unpubl. Rep., 21 p.
- \_\_\_\_\_ & CHEN, T.T. (1986): Zur Mineralogie von Cu-Ni(Co)-Pb-Ag-Hg-Erzen im Revier Schwarzleo bei Leogang, Salzburg, Österreich. *Mitt. Österr. Geol. Ges.* **78**, 125-148.
- PUTZ, H., PAAR, W.H. & SUREDA, R.J. (2002b): Talcusita,  $\text{Ti}_2\text{Cu}_3\text{FeS}_4$ , en las vetas epitermales de mina Capillitas, provincia de Catamarca, NW-Argentina. *6° Congreso de Mineralogía y Metalogenia (Buenos Aires), Artículos*, 361-364.
- \_\_\_\_\_, \_\_\_\_\_, \_\_\_\_\_ & ROBERTS, A.C. (2002a): Germanium mineralization at Capillitas, Catamarca Province, Argentina. *Int. Mineral. Assoc., 18<sup>th</sup> Gen. Meeting (Edinburgh), Abstr.*, 265.
- SASSO, A.M. (1997): *Geological Evolution and Metallogenetic Relationships of the Farallón Negro Volcanic Complex, NW Argentina*. Ph.D. thesis, Queen's University, Kingston, Ontario.
- \_\_\_\_\_ & CLARK, A.H. (1998): The Farallón Negro group, northwest Argentina: magmatic, hydrothermal and tectonic evolution and implications for Cu-Au metallogeny in the Andean back-arc. *SEG Newsletter* **34**, 1-18.
- SHELDRIK, G.M. (1997a): *SHELXS-97. A Computer Program for Crystal Structure Determination*. University of Göttingen, Göttingen, Germany.
- \_\_\_\_\_ (1997b): *SHELXL-97. A computer program for crystal structure refinement*. University of Göttingen, Göttingen, Germany.

- SÖHNGE, P.G. (1964): The geology of the Tsumeb mine. In *The Geology of Some Ore Deposits in Southern Africa* **2** (S.H. Haughton, ed.). Geological Society of South Africa, Johannesburg, South Africa (367-382).
- UNTERRICHTER VON RECHTENTHAL, J.F. & RANGE, K.J. (1978):  $\text{Ag}_8\text{GeTe}_6$ , ein Vertreter der Argyroditfamilie. *Z. Naturforsch.* **33b**, 866-872.
- WANG, NAIDING (1978): New data for  $\text{Ag}_8\text{SnS}_6$  (canfieldite) and  $\text{Ag}_8\text{GeS}_6$  (argyrodite). *Neues Jahrb. Mineral., Monatsh.*, 269-272.
- \_\_\_\_\_ (1988): Experimental study of the Cu-Ge-S ternary phases and their mutual relations. *Neues Jahrb. Mineral., Abh.* **159**, 137-151.
- \_\_\_\_\_ (1995): The Ag-Ge-S system: New experimental results. *Neues Jahrb. Mineral., Abh.* **169**, 313-317.
- \_\_\_\_\_ & VIAENE, W. (1974): The polymorphs of  $\text{Cu}_8\text{GeS}_6$  – a preliminary study. *Neues Jahrb. Mineral., Monatsh.*, 442-446.
- WEISBACH, A. (1886): Argyrodit, ein neues Silbererz. *Neues Jahrb. Mineral., Geol., Palaeont.* **II**, 67-71.
- YOUNG, B.B. & MILLMAN, A.P. (1964): Microhardness and deformation characteristics of ore minerals. *Inst. Mining Metall. Trans.* **73**, 437-466.

*Received February 6, 2004, revised manuscript accepted September 11, 2004.*